Constant Field Toroidal SMES Magnet

Alexey L. Radovinsky, Leslie Bromberg, Joseph V. Minervini, Philip C. Michael, Thomas Servais, Eric Forton, and Emma Pearson

***Abstract*—The Massachusetts Institute of Technology has been performing a preliminary study of superconducting magnetic energy storage (SMES) magnet configurations under a Pôle MecaTech Cluster collaboration sponsored by the government of the Walloon Region in Belgium. Consortium members include Ion Beam Applications S.A. (IBA), CE+T Power (CE+T), Euro-Diesel S.A. (Euro-Diesel), Jema S.A. (JEMA), the University of Liege (ULG), the Catholic University of Louvain-la-Neuve (UCL), and the Liege Space Center (CSL). The goal of the project was to assess the commercial feasibility of various SMES magnet configurations by evaluating specific energy, magnetic field shielding properties, and manufacturing cost. Among the examined configurations, the constant field toroid (CFT) attracted our attention, and it is the subject of this paper. The present study presents the description of the magnetic design algorithm and an example of the first-level optimization of the stored and specific energy. Numerical simulations are performed using Cobham Opera. A procedure of a simplified analytical optimization of a magnet system is used to maximize the stored energy or the specific energy (per unit weight of the conductor) of a CFT magnet.**

***Index Terms*—constant field toroidal magnet, SMES, superconducting magnetic energy storage.**

I. Introduction

ONE of the traditionally considered configurations of a SMES magnet [1], [2] is a toroid [3]–[5]. This configuration provides the best field containment and a very low level of stray fields, even at small distances from the magnet without the need for ferromagnetic shielding.

The main drawback of the conventional toroidal magnets comprised of multiple racetrack-shaped coils is the inverse relationship between magnetic field and the radius, r. The magnetic field peaks up at the outer side of the inner leg of the racetrack where it defines the working conditions of the superconductor. Then it decays as 1/r, resulting in rather inefficient space utilization, as the volume with high field is highly localized.

To mitigate this disadvantage, a toroidal magnet comprised of discrete graded coils creating an almost constant magnetic field in a large volume inside the magnet is considered here.

Manuscript received September 1, 2015; accepted December 11, 2015. Date of publication December 17, 2015; date of current version December 24, 2015. This work was supported by a Pôle MecaTech Cluster collaboration sponsored by the government of the Walloon Region in Belgium.

A. L. Radovinsky, L. Bromberg, J. V. Minervini, and P. C. Michael are with MIT Plasma Science and Fusion Center, Cambridge, MA 02139 USA (e-mail: radovinsky@psfc.mit.edu; brom@psfc.mit.edu; minervini@psfc.mit.edu; michael@psfc.mit.edu).

T. Servais, E. Forton, and E. Pearson are with Ion Beam Applications S.A. (IBA), 1348 Louvain-la-Neuve, Belgium (e-mail: Thomas.Servais@iba-group.com; Eric.Forton@iba-group.com; Emma.Pearson@iba-group.com).

Color versions of one or more of the figures in this paper are available online at http://ieeexplore.ieee.org.

Digital Object Identifier 10.1109/TASC.2015.2509246

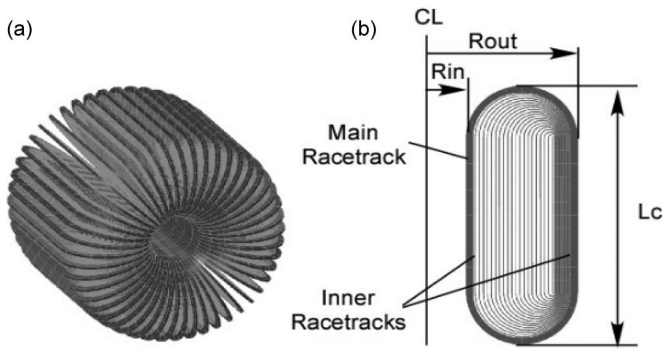

Fig. 1. CTF: (a) magnet; (b) individual TF coil.

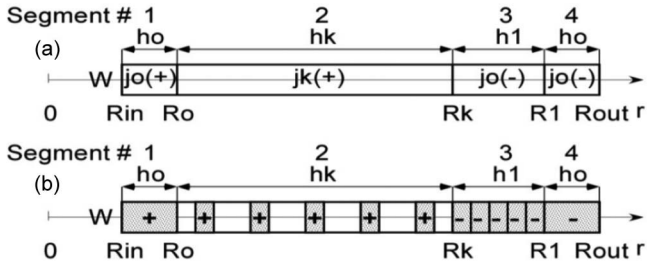

Fig. 2. Coil cross section (a) without and (b) with discretization.

Originally, "alternative toroid" design [6] was defined by Dr. Mohamed A. Hilal and his group in terms of a 1D axisymmetric radial function of a non-uniform current density distribution. Apparently, the untimely death of Dr. Hilal in the middle of this project precluded publishing their results. In the present study, this distribution is discretized both azimuthally and radially to be represented by a multiplicity of conventional racetracks. This discretization is closer to reality and leads to a more convenient for implementation constant current density distribution.

II. Definitions

Consider a coil system comprised of N Toroidal Field (TF) coils extending radially outward and evenly spaced in the circumferential direction. Fig. 1 depicts a magnet having $N = 48$ TF coils and a view of a single TF coil. Each TF coil is comprised of multiple racetracks arranged as described below.

The straight legs of the racetracks, which are parallel to the axis of the magnet, are arranged for the best compliance with the current distribution shown in the schematics in Fig. 2(a) and (b). Fig. 2(a) depicts the midplane cross section of a single racetrack assuming constant current densities.

In Fig. 2(a), W is the width of the racetrack winding. Rin and Rout are radial boundaries. There are four segments; which

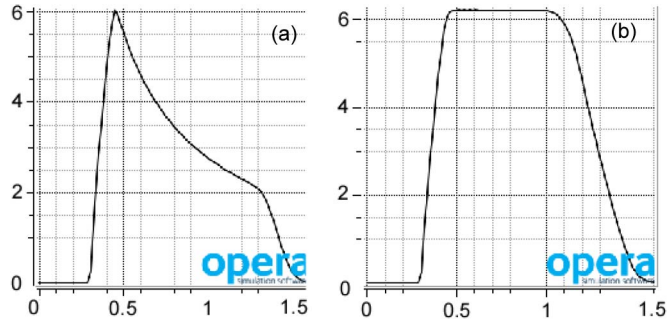

Fig. 3. B (in teslas) versus radius (in meters) at midplane in (a) SRT and (b) CFT magnets.

are $h0$, hk, $h1$ and $h0$ long in the radial direction, respectively. Current flows normal to the page. Respective current densities in the segments are $j0$, jk, $j0$ and $j0$, those marked by $(+)$ are opposite to those marked by $(-)$. Lengths ($h0$, hk, $h1$) and current densities ($j0$, jk) are scaled so that the total current in all bars is algebraically equal to zero.

The following parameters are given: $B0$—maximum target field in the system; $j0$—current density in segments 1, 3 and 4; N—number of TF coils; Rin and Rout—inner and outer radial boundaries of the coils; Lc—the axial extent of the coils.

System parameters may be calculated in the following sequence: $W \leq \text{Wmax} = \text{Rin}/2^*\text{Cot}(\pi/N)$, the width of the coil chosen to avoid overlapping in the left corners in Fig. 2(a); $h0 = \text{Rin}^*k/(1-k)$, where $k = 2^*\pi^*B0/(\mu0^*N^*W^*j0)$; $R0 = \text{Rin} + h0$, where $R0$ is the outer radius of segment 1; $\text{jk} = k^*j0$, where jk is the current density in segment 2; $\text{hk} = (\text{Rout} - R0 - h0)/(1+k)$, $h1 = k^*\text{hk}$ are the radial extents of segments 2 and 3, respectively.

Fig. 2(b) depicts discretization of the current distribution shown in Fig. 2(a). Segments 1 and 4 represent the opposite legs of the main racetrack. Segments 2 and 3 are broken up into equal numbers, m, of current legs of the inner racetracks, each with the same current density, $j0$. Discrete currents in Segment 2 are spaced evenly to better match the uniformity of jk.

III. Constant Field Versus Single Racetrack Toroids

First, let us compare a Constant Field Toroid comprised of the Main and Inner Racetracks with a Single Racetrack Toroid (SRT) comprised of Main Racetracks only. Unless specified differently, to minimize the number of variables in these and further models we assume that $B0 = 6.2$ T, $j0 = 50$ A/mm^2, $\text{Rin} = 0.3$ m, $\text{Rout} = 1.5$ m, $\text{Lc} = 3$ m, $N = 48$, $m = 20$, that the average density of the winding, $\text{dc} = 5700$ kg/m^3, and that coil windings touch at the ID, i.e. that $W = \text{Wmax}$. Fig. 3(a) and (b) depict the azimuthal components of the B-field calculated as a function of radius in the midplane for the SRT and CFT models similar to the one shown in Fig. 1(a).

Stored energy, Em, the weight of the conductor, Mc, and the specific stored energy defined as Em/Mc were calculated for the SRT and CFT models with the same as above characteristics as a function a variable inner radius, Rin, defined in 0.1 increments of Rin/Rout. The results are shown in respective Figs. 4–6.

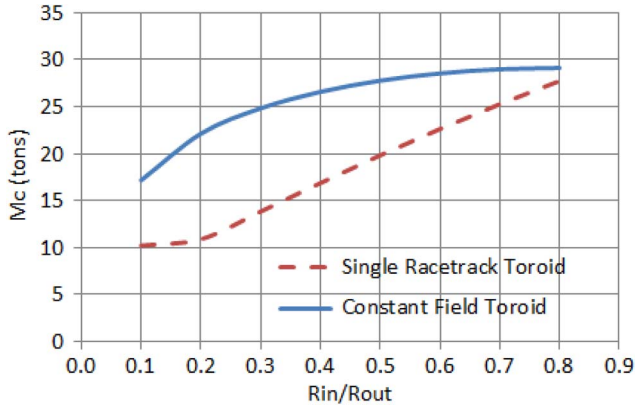

Fig. 4. Conductor weight versus Rin/Rout.

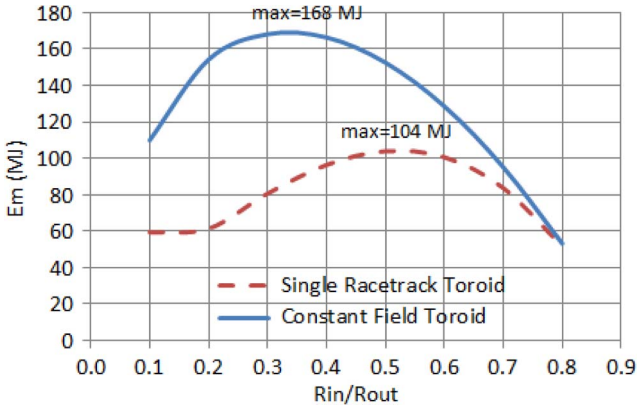

Fig. 5. Stored energy versus Rin/Rout.

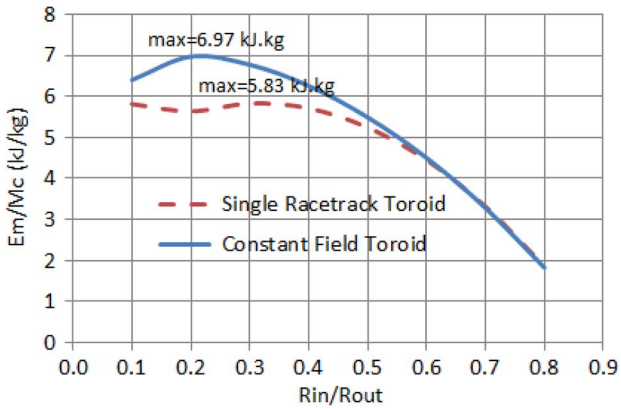

Fig. 6. Specific energy versus Rin/Rout.

Apparently, for this configuration the maxima of Em and Em/Mc occur at different values of Rin/Rout. Comparing these maxima shows that the CFT magnets have advantage by both parameters, 168 MJ$/104$ MJ $= 1.6$ times by the stored energy and 6.97 MJ/kg$/5.83$ MJ/kg $= 1.2$ times by Em/Mc.

IV. Analytical Optimization

The above example shows that quantitative characteristics of a CFT magnet have to be compared at their optima. This is done analytically using the following assumptions about the design of the magnet.

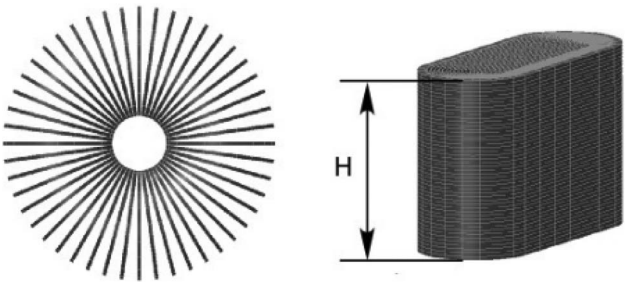

Fig. 7. Rearranging CFT coils into a stack.

A. Conductor

The requirements set by the project were that the SMES shall be inexpensive and suitable for working in the specified AC mode. These conditions led us to choosing a liquid He cooled NbTi Cable in Conduit Conductor (CICC for operating current, Iop = 6 kA, peak field, Bmax = 6.2 T, smeared over winding pack current density, Jwp = 52 A/mm^2) for all, the Main, and Inner racetracks. The SC cable is comprised of 60 (20 composite with 62% fraction of copper and 40 copper) 1.0-mm diameter strands twisted into a 3-stage $(3 \times 4 \times 5)$ cable and placed into a 10 mm by 10 mm, 0.7-mm thick wall steel jacket filled with liquid He at 4.2 K. Thickness of the turn insulation is 0.3 mm. The smeared density of the winding is 5700 kg/m^3.

This design verified using a CICC Design Tool [7] proved to withstand the specified AC losses leading to a 4.6 K operating temperature with a 1.2 K temperature margin at a 0.46 fraction of critical. Quench protection at the $Em = 168$ MJ by fast discharge on an external 0.81 ohm resistor leads to the maximum adiabatic temperature rise to 150 K and the maximum terminal voltage of 4.9 kV.

B. Conductor Weight and Magnet Stored Energy

The weight of the conductor, Mc, and total stored energy, E_m, can be calculated using the following formulae

$$Mc = D_c * V_c, \quad E_m = \frac{B_0^2}{2\mu_0} V_{CF}.$$

Here $V_c = H * A$ is the volume of the winding, D_c is its average density and $H = 2\pi R_{in}$ is the height of the stack in Fig. 7; A is the area of the conductor in the axial-radial cross section of the TF coil; V_{CF} is the toroidal constant field volume.

Respective formulae for calculating non-dimensional volumes, $\tilde{V}_c = V_c/R_{out}^3$ and $\tilde{V}_{CF} = \gamma V_{CF}/R_{out}^3$, as a function of non-dimensional parameters, $\alpha = R_{in}/R_{out}$, $\beta = L_c/R_{out}$, $k = (B_0/\mu_0 j_0 R_{in})$, are

$$\tilde{V}_c = 2\pi\alpha \left\{ \frac{2k}{1+k}(\alpha+\beta-1) + \frac{\pi}{4}\left[(1-\alpha)^2 - \frac{1-k}{1+k}\left(1 - \frac{1+k}{1-k}\alpha\right)^2\right]\right\}$$

$$\tilde{V}_{CF} = \gamma 2\pi \left[\left(\frac{1}{1+k}\right)^2 - \left(\frac{\alpha}{1-k}\right)^2\right] \times \left[(\alpha+\beta-1) + \frac{\pi}{4}\left(\frac{1}{1+k} - \frac{\alpha}{1-k}\right)\right].$$

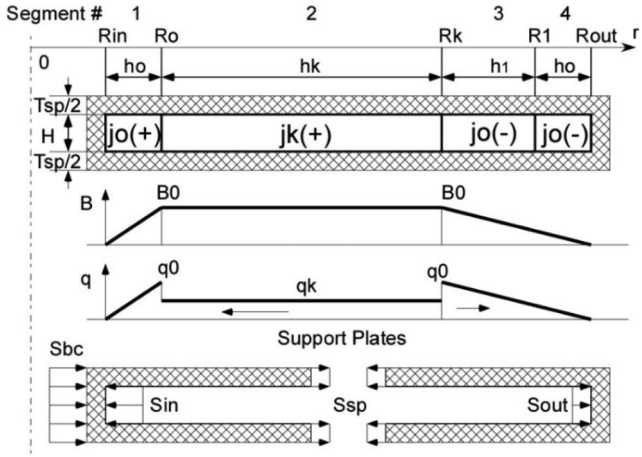

Fig. 8. Sizing TF coil support plates.

Here $\gamma = 1.2$ is a numerically defined adjustment coefficient, accounting for the transitional volumes between $B = 0$ to $B = B0$.

Comparing with the precise values calculated using 3D modeling by Opera[1] showed that these formulae have a 1% and 10% margin of error for the conductor volume and the stored energy respectively.

C. Structural Characteristics

To evaluate the weight of the cold structure let us assume that the winding of a TF coil is contained in a steel case and that all TF coils are wedged together at the ID as in the ITER TF structure [8]. The walls of the case are to be designed to withstand significant radial forces tending to widen the coil in the radial direction. Significantly smaller axial forces are contained by the self-supporting end turns of the racetracks formed by the CICC conductor. To the first approximation the thickness of the plates can be evaluated using a 1D model shown in Fig. 8. It is similar to the one shown in Fig. 2(a) except for here we bundle up all the coils into a single stack as shown in Fig. 7. The hashed frame of the coil stack represents the support plates of the equivalent thickness, Tsp. (For each of N racetrack TF coils this is equivalent to two structural face plates, Tsp/N/2 thick each.)

Diagrams in Fig. 8 depict theoretical 1D distributions of the normal to the plane of the coil field, B(r), and the volumetric density of the Lorentz force, q(r), defining the integrated radial stresses, S, in the coil winding. Here

$$q_0 = j_0 B_0, \quad q_k = j_k B_0$$

$$S_{in} = q_k h_k + \frac{q_0 h_0}{2}, \quad S_{out} = \frac{1}{2} q_0 (h_0 + h_1)$$

$$S_{bc} = S_{in} - S_{out} = q_k h_k = \frac{q_0 h_1}{2}, \quad S_{sp} = S_{out}\frac{H}{T_{sp}}.$$

Using non-dimensional notation introduced above these stresses can be presented in the following form:

$$S_{in} = q_0 R_{out} k \left[\frac{1}{1+k} - \frac{\alpha}{2(1-k)}\right], \quad S_{out} = q_0 R_{out}\frac{k}{2(1+k)}$$

$$S_{bc} = q_0 R_{out}\frac{k}{2}\left(\frac{1}{1+k} - \frac{\alpha}{1-k}\right), \quad S_{sp} = q_0 R_{out}\frac{k}{2(1+k)}\frac{H}{T_{sp}}.$$

[1]Cobham Opera, Computer Program. [Online]. Available: www.cobham.com

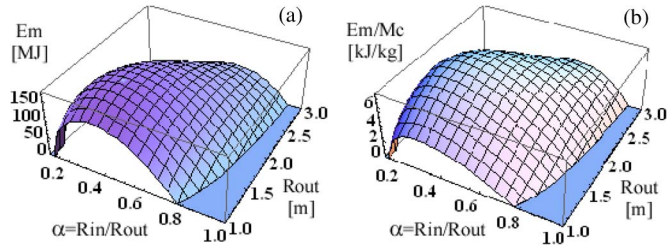

Fig. 9. (a) Stored energy Em and (b) specific energy Em/Mc versus (R_{out}, α), for $V_{env} = 27$ m^3.

Assuming that stresses in the support plates shall not exceed the allowable stress, Sm, [9] we can find the minimum equivalents thickness

$$T_{sp} = \frac{q_0 R_{out} H}{S_m} \frac{k}{2(1+k)}, \quad \text{where } H = 2\pi R_{in}.$$

This formula is used in the next section to calculate the total weight of the support plates of the TF cases.

D. Analytical Optimization

A simplified optimization procedure described in this section may be used for the first-level optimization instrumental for estimating the parameters of a magnet system as a function of its stored energy.

Fig. 9 generated using Mathematica[2] depict Stored Energy, Em, and Specific Energy, Em/Mc, calculated using analytical formulae derived in the previous section. The surfaces are generated in the space of two variable parameters, R_{out} and $\alpha = R_{in}/R_{out}$, for a given volume of a rectangular envelope, $V_{env} = L_c(2R_{out})^2 = 27$ m^3 of the magnet. This way the main defining parameters are derived as $R_{in} = \alpha R_{out}$, $L_c = V_{env}/(2R_{out})^2$, $k = B_0/(\mu_0 j_0 R_{in})$.

As shown in Fig. 9 both functions, Em and Em/Mc, have distinct maxima in the (R_{out}, α) parametric space.

Major characteristics of the magnets optimized using this procedure for four given envelope volumes are shown in Table I. The total weight, M, of the magnet including the conductor, the cold mass structure and the cryostat were used for calculating its specific energy, Em/M.

These results show that the specific stored energy increases with the size of the system. They also show that the parameters of systems optimized by, Em and Em/Mc, on the average differ by about 10%.

Note that this optimization procedure is independent of the number of discrete coils. It can be used to develop a system with a large number of thin coils or with a small number of thick coils.

V. Conclusion

An alternative design of a high energy density toroidal magnet system with a large toroidal constant magnetic field volume is described in this paper.

[2]Mathematica, Computer Program. [Online]. Available: www.wolfram.com

TABLE I
Optimized CFT Magnets

Venv (m3)	α	Rin (m)	Rout (m)	Lc (m)	M (t)	Em (MJ)	Em/M (kJ/kg)
Optimized by Max(Em)							
8	0.38	0.44	1.15	1.51	13.6	35	2.60
27	0.35	0.56	1.58	2.72	35.8	171	4.77
64	0.33	0.66	1.98	4.07	71.1	478	6.72
125	0.32	0.76	2.38	5.53	121.6	1031	8.48
Optimized by Max(Em/Mc)							
8	0.34	0.44	1.29	1.20	12.6	33	2.64
27	0.30	0.58	1.95	1.78	31.5	154	4.89
64	0.27	0.71	2.63	2.31	60.3	417	6.92
125	0.25	0.82	3.34	2.81	100.7	877	8.71

An algorithm of numerical analyses of a Constant Field Toroidal SMES is developed and used for optimization of the coil system.

Several different configurations of a SMES were considered for the future detailed development in the framework of the project. Even though the CFT was shown to be superior to the SRT and other solenoidal SMES configurations, we decided not to pursue it. The CFT was rejected primarily due to the complexity of its design leading to a significantly higher cost of manufacturing. It was noted however, that there may be projects, in which certain properties of this design can give it an advantage.

Acknowledgment

This study is dedicated to the memory Dr. Mohamed A. Hilal, the original author of the concept of a Constant Field Toroid.

References

[1] C. Luongo, "Superconducting storage systems: An overview," *IEEE Trans. Magn.*, vol. 32, no. 4, pp. 2214–2223, Jul. 1996.
[2] P. Tixador, "Superconducting magnetic energy storage: Status and perspective," in *Proc. IEEE/CSC ESAS European Supercon. News Forum*, Jan. 2008, vol. 3, pp. 1–14.
[3] M. Takeo *et al.*, "Plans on developments of a SMES system in Kyushu," *Fusion Eng. Des.*, vol. 20, pp. 385–388, Feb. 1993.
[4] M. Yamamoto *et al.*, "Development of elementary technologies for 100 kWh/20 MW SMES with multipurpose applications," in *Proc. IEEE Power Eng. Soc. Meet.*, 2000, pp. 2716–2721.
[5] C. Luongo, "Optimization of toroidal superconducting magnetic energy storage magnets," *Phys. C, Supercond.*, vol. 324, no. 1–4, pp. 101–114, May 2001.
[6] A. Husseiny, Z. Sabri, and Y. Eyssa, "A prototype of a Superconductive Magnetic Energy Storage (SMES) system for Air Force use," Air Force Development Test Center, Tyndall AFB, FL, USA, Contract F08635-92-C-0072, M. A. Hilal, Jul. 1992–Apr. 1993.
[7] A. E. Long, *Cable-in-Conduit Superconductor Design Tool*. Cambridge, MA, USA: MIT Press, 1993.
[8] C. Sborchia, "Design and specifications of the ITER TF coils," *IEEE Trans. Appl. Supercond.*, vol. 18, no. 2, pp. 463–466, Jun. 2008.
[9] J. W. Sa *et al.*, "Mechanical characteristics of austenitic stainless steel 316LN weldments at cryogenic temperature," in *Proc. 21st IEEE/NPS Symp. Fusion Eng.*, Sep. 2005, pp. 1–4.